# Neutron Diffraction Study on Lanthanum Gallate Perovskite Compound Series

Masahiro Kajitani,[†] Motohide Matsuda,[†] Akinori Hoshikawa,[‡] Ken-ichi Oikawa,[‡] Shuki Torii,[‡] Takashi Kamiyama,[‡] Fujio Izumi,[§] and Michihiro Miyake*[,†]

*Department of Environmental Chemistry and Materials, Faculty of Environmental Science and Technology, Okayama University, Tsushima-Naka, Okayama 700-8530, Japan, Institute for Materials Structure Science, High Energy Accelerator Research Organization, Tukuba, Ibaraki 305-0801, Japan, and Advanced Materials Laboratory, National Institute for Materials Science, Tsukuba, Ibaraki 305-0044, Japan*

*Received March 18, 2003. Revised Manuscript Received June 12, 2003*

The crystal structures of lanthanum gallate perovskite compounds, $LaGaO_3$, $LaGa_{0.8}Mg_{0.2}O_{2.9}$, and $La_{0.8}Sr_{0.2}Ga_{0.8}Mg_{0.2}O_{2.8}$ which is well-known as a superior oxide ion conductor, have been analyzed by neutron powder diffraction to clarify the effect of the substitutions on the perovskite structures. The crystal structure of $Mg^{2+}$-substituted $LaGaO_3$, $LaGa_{0.8}Mg_{0.2}O_{2.9}$, belongs to the same orthorhombic space group, *Pbnm*, as that of $LaGaO_3$, and the oxygen vacancies were found to be created at the planar O2 atom sites of $GaO_6$ octahedron. On the other hand, the crystal structure of doubly $Sr^{2+}$- and $Mg^{2+}$-substituted $LaGaO_3$, $La_{0.8}Sr_{0.2}Ga_{0.8}Mg_{0.2}O_{2.8}$, belongs to the cubic space group $Pm\bar{3}m$ and the oxygen vacancies were found to be in disorder. The distortion in the perovskite structures and the oxide ion conduction mechanism are discussed on the basis of the analytical results, together with the results of X-ray diffraction and total conductivity up to 800 °C.

## Introduction

In recent years, doubly $Sr^{2+}$- and $Mg^{2+}$-substituted $LaGaO_3$ (LSGM: $La_{1-x}Sr_xGa_{1-y}Mg_yO_{3-0.5x-0.5y}$), which has perovskite structure, has attracted a great deal of attention as a solid electrolyte of solid oxide fuel cells (SOFCs) because of its high oxide ion conductivity.[1−9] The oxide ion conductivity of LSGM at 800 °C is comparable to that of 8 mol % yttria stabilized zirconia (8 mol % YSZ) at about 1000 °C. Hence, the SOFC with an operating temperature at 800 °C or below can be realized by using the LSGM as a solid electrolyte.[10,11]

The structural analysis brings valuable information to clarifying the ion conduction mechanism, because the ion-conducting property is strongly dependent on the crystal structure, especially vacancy sites. The structural changes of $LaGaO_3$ (LG) and $La_{0.9}Sr_{0.1}Ga_{0.8}Mg_{0.2}O_{2.85}$ (LSGM9182) as a function of temperature have been investigated independently by Slater et al.[12,13] and Lerch et al.[14] The different results were, however, derived with each other. Slater et al. reported the following results from powder neutron diffraction study. The crystal structure of LG belongs to the orthorhombic space group *Pbnm* at room temperature, and to the rhombohedral space group *R*3*c* with noncentrosymmetry above 250 °C. The crystal structure of LSGM9182 belongs to the monoclinic space group *I*2/*a* at ambient temperature, and to the rhomboheral space group *R*3*c* at 1000 °C via two phase transitions above 250 °C, i.e., monoclinic (pseudo-orthorhombic) → monoclinic (pseudo-rhombohedral) → rhombohedral. On the other hand, Lerch et al. concluded the following from their powder neutron diffraction study. Although the crystal structure of LG belongs to the orthorhombic space group *Pbnm* at ambient temperature, it belongs to the rhombohedral space group $R\bar{3}c$ with centrosymmetry at 800 °C. The crystal structure of LSGM9182 belongs to the orthorhombic space group *Imma* at room temperature, and to the cubic space group $Pm\bar{3}m$ at 800 °C. Thus, because the crystal structures of LSGM and LG have not yet been clearly solved, the results reported are unavailable for discussing the oxide ion conduction mechanism of LSGM.

* To whom correspondence should be addressed. E-mail: mmiyake@cc.okayama-u.ac.jp.
[†] Okayama University.
[‡] High Energy Accelerator Research Organization.
[§] National Institute for Materials Science.

(1) Ishihara, T.; Matsuda, H.; Takita, Y. *J. Am. Ceram. Soc.* **1994**, *116*, 3801.
(2) Feng, M.; Goodenough, J. B. *Eur. J. Inorg. Chem.* **1994**, *31*, 663.
(3) Ishihara, T.; Matsuda, H.; Takita, Y. *Solid State Ionics* **1995**, *79*, 147.
(4) Huang, K.; Feng, M.; Goodenough, J. B. *J. Am. Ceram. Soc.* **1996**, *79*, 1100.
(5) Huang, P.; Petric, A. *J. Electrochem. Soc.* **1996**, *143*, 1644.
(6) Huang, K.; Ticky, R. S.; Goodenough, J. B. *J. Am. Ceram. Soc.* **1998**, *81*, 2565.
(7) Huang, K.; Ticky, R. S.; Goodenough, J. B. *J. Am. Ceram. Soc.* **1998**, *81*, 2576.
(8) Khan, M. S.; Islam, M. S.; Bates, D. R. *J. Phys. Com. B* **1998**, *102*, 3099.
(9) Islam, M. S. *Solid State Ionics* **2002**, *154*−*155*, 75.
(10) Huang, K.; Ticky, R. S.; Goodenough, J. B. *J. Am. Ceram. Soc.* **1998**, *81*, 2581.
(11) Matsuda, M.; Ohara, O.; Murata, K.; Ohara, S.; Fukui, T.; Miyake, M. *Electrochem. Solid-State Lett.* **2003**, *6*, A140.
(12) Slater, P. R.; Irvine, J. T. S.; Ishihara, T.; Takita, Y. *J. Solid State Chem.* **1998**, *139*, 135.
(13) Slater, P. R.; Irvine, J. T. S.; Ishihara, T.; Takita, Y. *Solid State Ionics* **1998**, *107*, 319.
(14) Lerch, M.; Boysen, H.; Hansen, T. *J. Phys. Chem. Solids* **2001**, *62*, 445.

10.1021/cm030294y CCC: $25.00 
Published on Web 08/08/2003

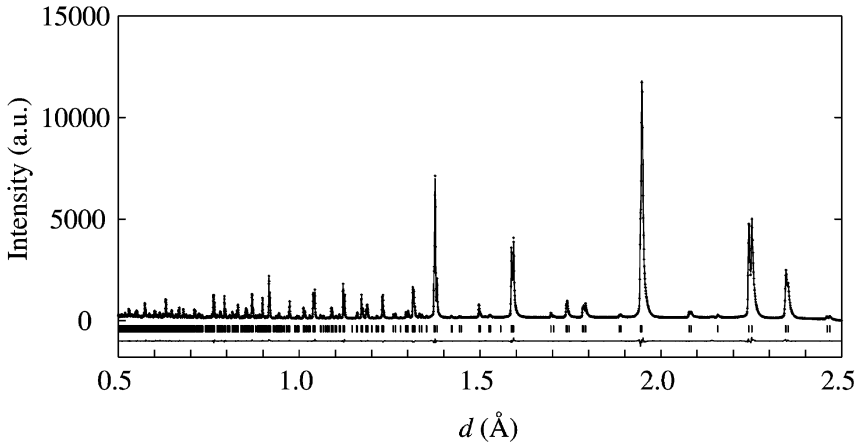


**Figure 1.** Observed (plus signs), calculated (solid line), and difference (solid line on the bottom) patterns for TOF neutron powder diffraction data of $LaGaO_3$ at room temperature.

Moreover, the effects of substituting $Sr^{2+}$ and $Mg^{2+}$ ions on the perovskite structures and ion-conducting properties of $LaGaO_3$-based solid solutions have been investigated very little. It is of significance to systematically investigate the effects, because the investigation brings the useful information to examine the oxide ion conduction mechanism. Thus, we have studied the relationship between the crystal structures and ion-conducting properties of the following solid solutions: LG; $La_{0.8}Sr_{0.2}GaO_{2.9}$ (LSG82), where $Sr^{2+}$ ions are substituted for 20 mol % of $La^{3+}$ ions in the A site; $LaGa_{0.8}Mg_{0.2}O_{2.9}$ (LGM82), where $Mg^{2+}$ ions are substituted for 20 mol % of $Ga^{3+}$ ions in the B site; and $La_{0.8}Sr_{0.2}Ga_{0.8}Mg_{0.2}O_{2.8}$ (LSGM8282), where $Sr^{2+}$ and $Mg^{2+}$ ions are doubly substituted for 20 mol % of $La^{3+}$ ions and 20 mol % of $Ga^{3+}$ ions, respectively. In this paper, we report the structural analyses of these compounds by Rietveld method based on high-resolution neutron powder diffraction data at room temperature. Neutron diffraction is a useful means for precisely determining the positions and site occupancies of light elements such as O atom in compounds containing heavy elements.

## Experimental

LG, LSG82, LGM82, and LSGM8282 were prepared by solid-state reaction, using $La_2O_3$ (99.99%, Kanto), $SrCO_3$ (99.9%, Kanto), $Ga_2O_3$ (99.9%, Kojundo), and MgO (99.0%, Kanto) as starting materials. Before weighing, the $La_2O_3$ powders were preheated at 1000 °C for 5 h in air to remove adsorbed water. The starting materials weighted with stoichiometry were mixed, ground in a mortar for 1 h, and then calcinated at 1100 °C for 10 h in air. After the calcination, the mixture was shaped into pellets under 40 MPa, and then fired at 1500 °C for 10 h in air. The products were identified by powder X-ray diffraction (XRD), and their structural changes were examined by high-temperature XRD, using a Rigaku RINT2100/PC diffractometer with monochromated Cu Kα radiation and equipped with an electric furnace.

The neutron diffraction data were measured on a time-of-flight (TOF) neutron diffractometer at room temperature, using *Sirius* with high-resolution (ca. $1.0 \times 10^{-3}$ in $\Delta d/d$) at the pulsed spallation neutron facility KENS, High Energy Accelerator Research Organization, in Japan. The sample of ca. 10 g was loaded in a vanadium tube under atmospheric pressure, and set on the diffractometer. The data collection was made by an array of 320 position-sensitive detectors installed in a backward bank with the range $150 \leq 2\theta/° \leq 175$. The observed data as a function of time were converted into those as a function of $d$ values, referring to intensity data observed in a separate measurement of Si powder as a standard sample.

Total conductivity measurements were carried out by an ac two-probe impedance method over a frequency range of 5 to 13 MHz up to 900 °C in air at an ac voltage with amplitude of 10 mV for all temperatures and all frequencies, using a Hewlett-Packard 4192A impedance analyzer. The two electrodes were formed by applying platinum paste to the two ends of the pellet and then firing it at 1100 °C for 1 h in air.

## Results and Discussion

The XRD revealed that LG, LGM82, and LSGM8282 prepared were single phases, although LSG82 coexisted with a small amount of $LaSrGa_3O_7$ as an impurity phase. The single phase of LSG82 could not be yielded even by repeated heating treatments. From the results, the solid solution of $Sr^{2+}$ ions in $La_{1-x}Sr_xGaO_{3-x/2}$ was guessed to be limited to $x = 0.1$, as indicated in the previous papers.[1,15] The structural analysis of LSG82 prepared here, therefore, was abandoned.

The collected diffraction data in the range $0.5 \leq d/Å \leq 2.5$ were analyzed by Rietveld method, using the program RIETAN-2001T for TOF neutron diffraction.[16,17] In the refinement, the constraint was applied to the site occupancy factor, except for O atoms in LGM82 and LSGM8282, assuming that the composition ratios in the specimens were ideal values expected from the batch compositions. The structural data by Marti et al. were adopted as initial parameters for LG,[18] because XRD indicated that LG crystallized in the orthorhombic space group *Pbnm*, and the structure refinement was performed on applying isotropic temperature factors. The observed and calculated diffraction patterns of LG are shown in Figure 1, and the final structural parameters are listed in Table 1. The resulting parameters are in good agreement with those previously reported.[12−14,18,19]

(15) Anderson, P. S.; Mather, G. S.; Marques, F. M. B.; Sinclair, D. C.; West, A. R. *J. Euro. Ceram. Soc.* **1999**, *19*, 1665.
(16) Ohta, T.; Izumi, F.; Oikawa, K.; Kamiyama, T. *Physica B* **1997**, *234−236*, 1093.
(17) Izumi, F.; Ikeda, T. *Mater. Sci. Forum* **2000**, *321−324*, 198.
(18) Marti, W.; Fischer, P.; Altorfer, F.; Scheel, H. J.; Tadin, M. *J. Phys. Condens. Matter* **1994**, *6*, 127.
(19) Howard, C. J.; Kennedy, B. J. *J. Phys. Condens. Matter* **1999**, *11*, 3229.

**Table 1. Structural Parameters and Final *R* Values for $LaGaO_3$, $LaGa_{0.8}Mg_{0.2}O_{2.9}$ and $La_{0.8}Sr_{0.2}Ga_{0.8}Mg_{0.2}O_{2.8}$[a]**

| | $LaGaO_3$ | $LaGa_{0.8}Mg_{0.2}O_{2.9}$ | $La_{0.8}Sr_{0.2}Ga_{0.8}Mg_{0.2}O_{2.8}$ |
|---|---|---|---|
| crystal structure | orthorhombic | orthorhombic | cubic |
| space group | *Pbnm* | *Pbnm* | $Pm\bar{3}m$ |
| *a* (Å) | 5.52432(2) | 5.5474(1) | 3.91479(1) |
| *b* (Å) | 5.49249(2) | 5.5142(1) | |
| *c* (Å) | 7.77435(3) | 7.8229(1) | |
| *V* (Å$^3$) | 235.891(2) | 239.297(5) | 59.996(1) |
| La/Sr position | 4c | 4c | 1b |
| occupancy | 1.0 | 1.0 | 0.8/0.2 |
| *x* | −0.0037(1) | −0.0019(3) | 1/2 |
| *y* | −0.0168(1) | 0.0063(6) | 1/2 |
| *z* | 1/4 | 1/4 | 1/2 |
| $U_{iso}$ (Å$^2$) | 0.0041(1) | 0.0126(2) | 0.0177(3) |
| Ga/Mg position | 4b | 4b | 1a |
| occupancy | 1.0 | 0.8/0.2 | 0.8/0.2 |
| *x* | 1/2 | 1/2 | 0 |
| *y* | 0 | 0 | 0 |
| *z* | 0 | 0 | 0 |
| $U_{iso}$ (Å$^2$) | 0.0029(1) | 0.0041(2) | 0.0067(3) |
| O1 position | 4c | 4c | 3d |
| occupancy | 1.0 | 1.01(2) | 0.85(7) |
| *x* | 0.0668(1) | 0.0639(4) | 1/2 |
| *y* | 0.5068(2) | 0.5002(8) | 0 |
| *z* | 1/4 | 1/4 | 0 |
| $U_{iso}$ (Å$^2$) | 0.0051(1) | 0.0071(3) | 0.0477(4) |
| O2 position | 8d | 8d | |
| occupancy | 1.0 | 0.94(3) | |
| *x* | −0.2299(1) | −0.2579(6) | |
| *y* | 0.2290(1) | 0.2587(5) | |
| *z* | 0.0358(1) | 0.0368(2) | |
| $U_{iso}$ (Å$^2$) | 0.0058(1) | 0.0252(4) | |
| $R_{wp}$ | 3.46 | 5.05 | 6.44 |
| $R_p$ | 2.99 | 4.16 | 5.01 |
| $R_B$ | 1.06 | 3.02 | 4.95 |
| *S* | 1.34 | 2.21 | 2.88 |

[a]

$$R_{wp} = \left[\frac{\sum_i w_i\{y_i - f_i(x)\}^2}{\sum_i w_i y_i^2}\right]^{1/2}, \quad R_p = \frac{\sum_i |y_i - f_i(x)|}{\sum_i y_i}, \quad R_B = \frac{\sum_k |I_k(\text{“}o\text{”}) - I_k(c)|}{\sum_k I_k(\text{“}o\text{”})}, \quad S = \frac{R_{wp}}{R_e}, \quad B_{iso} = 8\pi^2 U_{iso}$$

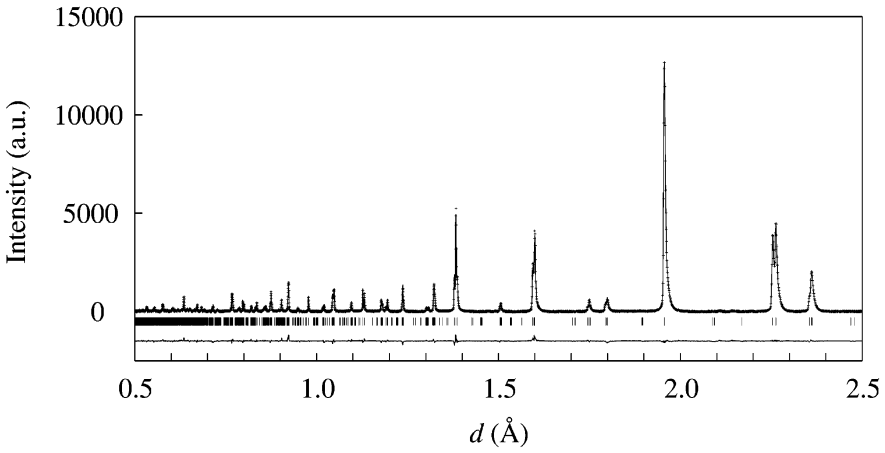


**Figure 2.** Observed (plus signs), calculated (solid line), and difference (solid line on the bottom) patterns for TOF neutron powder diffraction data of $LaGa_{0.8}Mg_{0.2}O_{2.9}$ at room temperature.

In the refinements of LGM82, the site occupancy factor of the Ga atom was fixed according to the chemical composition, parameters for the Mg atom were reset by using those for the Ga atom, and the site occupancy factors of O atoms were employed as parameters. The final parameters for LG refined here were adopted as initial parameters for LGM82, because XRD revealed that LGM82 was isostructural with LG. The observed and calculated diffraction patterns of LGM82 are shown in Figure 2, and the final structural parameters are listed in Table 1. It was found that introducing the $Mg^{2+}$ ion in the B site led the cell dimensions to

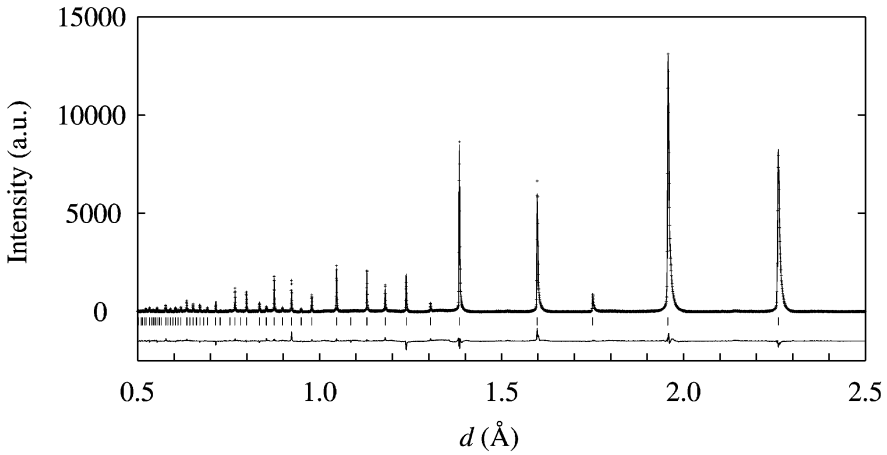


**Figure 3.** Observed (plus signs), calculated (solid line), and difference (solid line on the bottom) patterns for TOF neutron powder diffraction data $La_{0.8}Sr_{0.2}Ga_{0.8}Mg_{0.2}O_{2.8}$ at room temperature.

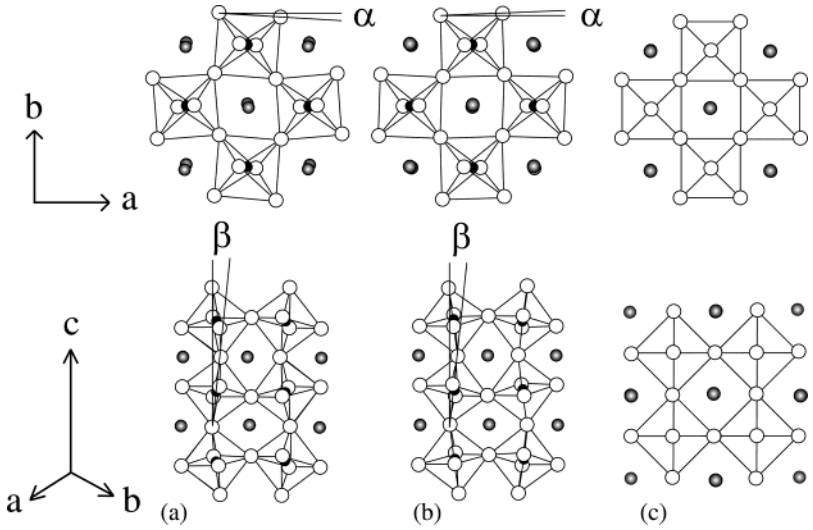


**Figure 4.** Comparison among the crystal structures of (a) $LaGaO_3$, (b) $LaGa_{0.8}Mg_{0.2}O_{2.9}$, and (c) $La_{0.8}Sr_{0.2}Ga_{0.8}Mg_{0.2}O_{2.8}$. α and $\beta$ denote tilt angles of $GaO_6$ octahedron around the *b* and *c* axes, respectively. The structure of $La_{0.8}Sr_{0.2}Ga_{0.8}Mg_{0.2}O_{2.8}$ is described according to orthorhombic cell.

expand, and preferentially created the oxygen vacancies at the planar O2 atom sites of $GaO_6$ octahedron for requiring electrical compensation, because the site occupancy factors of O1 and O2 atoms were close to 1.0 and 0.95, respectively, which were supposed from the chemical composition.

Any superstructure reflections that existed on the pattern of LSGM9182[12−14] could not be observed on that of LSGM8282. The crystal structure of LSGM8282 was, therefore, refined in the cubic space group $Pm\bar{3}m$. The site occupancy factors of La and Ga atoms were fixed according to the chemical composition, the parameters for Sr and Mg atoms were reset by using those for La and Ga atoms, respectively, and the site occupancy factors of O atoms were employed as parameters. Consequently, this model led the final R factor to the goodness, showing good agreement between the observed and calculated patterns as illustrated in Figure 3. Thus, it was decided the structure of LSGM8282 prepared here belongs to the same cubic space group, $Pm\bar{3}m$, as the ideal perovskite structure, i.e., the proto-perovskite structure. The crystal structure of LSGM seems to be dependent on the substituted amount of $Sr^{2+}$ ions for $La^{3+}$ ions in LGM82. The final structural parameters are listed in Table 1. The site occupancy factor of O atom was close to 0.93 expected from the chemical composition. Consequently, it was found that the oxygen vacancies in LSGM8282, whose quantity was twice as much as those in LGM82, were in disorder, whereas those in LGM82 were at the O2 atom sites.

Table 2 shows the selected interatomic distances of LG, LGM82, and LSGM8282. The $GaO_6$ octahedra in LG and LGM82 are close to the regular one, and the mean Ga−O bond length in LGM82 is slightly lengthened by replacing $Ga^{3+}$ ions with $Mg^{2+}$ ions. The $GaO_6$ octahedron in LSGM8282 is, however, the regular one with the Ga−O bond length shorter than the mean values in LG and LGM82 despite introducing $Sr^{2+}$ and $Mg^{2+}$ ions, whose ionic radii are larger than those of $La^{3+}$ and $Ga^{3+}$ ions, respectively. This was elucidated to be due to the fact that the distortion in the perovskite structure was removed by the transformation from the orthorhombic to the cubic as mentioned below. Slater et al. also reported that the Ga−O bond length was shortened in LSGM9182 at 1000 °C, and interpreted that the result was ascribed to the ascent of symmetry.[12] The Ga−O bond length of LSGM8282 is close to that analyzed by Huang et al.[6] The order of mean La−O bond lengths corresponds to that of cell volumes, i.e., LG < LGM82 < LSGM8282.

**Table 2. Selected Interatomic Distances (Å) of $LaGaO_3$, $LaGa_{0.8}Mg_{0.2}O_{2.9}$, and $La_{0.8}Sr_{0.2}Ga_{0.8}Mg_{0.2}O_{2.8}$**

| | $LaGaO_3$ | $LaGa_{0.8}Mg_{0.2}O_{2.9}$ | $La_{0.8}Sr_{0.2}Ga_{0.8}Mg_{0.2}O_{2.8}$ |
|---|---|---|---|
| La−O1 | 2.418(1) | 2.430(3) | 2.76820(2) |
| La−O1 | 2.646(1) | 2.748(6) | |
| La−O1 | 2.902(1) | 2.814(6) | |
| La−O2 | 2.482(1) | 2.534(3) | |
| La−O2 | 2.625(1) | 2.595(3) | |
| La−O2 | 2.821(1) | 2.923(3) | |
| mean La−O | 2.649 | 2.674 | 2.768 |
| Ga−O1 | 1.9786(1) | 1.9879(4) | 1.95740(1) |
| Ga−O2 | 1.971(1) | 1.975(3) | |
| Ga−O2 | 1.976(1) | 1.980(3) | |
| mean Ga−O | 1.975 | 1.981 | 1.957 |
| O1−O2 | 2.780(1) | 2.774(4) | 2.76820(2) |
| O1−O2 | 2.791(1) | 2.783(4) | |
| O1−O2 | 2.802(1) | 2.821(3) | |
| O1−O2 | 2.806(1) | 2.837(3) | |
| O2−O2 | 2.7552(1) | 2.7587(2) | |
| O2−O2 | 2.8279(2) | 2.834(1) | |
| mean O−O | 2.794 | 2.801 | 2.768 |

**Table 3. Tilt Angles (°) of $GaO_6$ Octahedron and Tolerance Factor of $LaGaO_3$, $LaGa_{0.8}Mg_{0.2}O_{2.9}$, and $La_{0.8}Sr_{0.2}Ga_{0.8}Mg_{0.2}O_{2.8}$**

| | $LaGaO_3$ | $LaGa_{0.8}Mg_{0.2}O_{2.9}$ | $La_{0.8}Sr_{0.2}Ga_{0.8}Mg_{0.2}O_{2.8}$ |
|---|---|---|---|
| tilt angle α | 9.3 | 3.8 | 0.0 |
| tilt angle $\beta$ | 15.0 | 14.3 | 0.0 |
| tolerance factor | 0.948 | 0.954 | 1.000 |

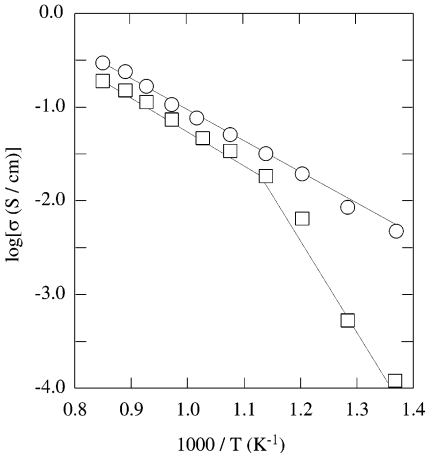


**Figure 5.** Temperature dependences of oxide ion conductivities of $LaGa_{0.8}Mg_{0.2}O_{2.9}$ (open square) and $La_{0.8}Sr_{0.2}Ga_{0.8}Mg_{0.2}O_{2.8}$ (open circle).

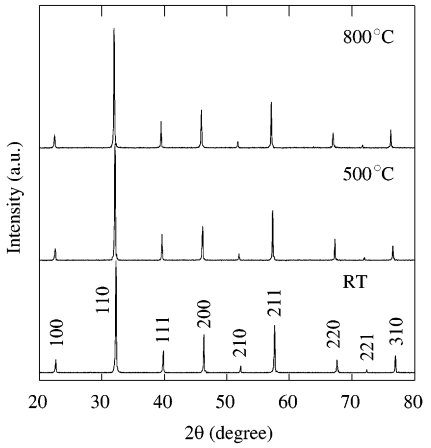


**Figure 6.** XRD patterns of $La_{0.8}Sr_{0.2}Ga_{0.8}Mg_{0.2}O_{2.8}$ as a function of temperature.

The distortions in LG, LGM82, and LSGM8282 from the ideal perovskite structure were discussed from the standpoint of the $GaO_6$ octahedral tilt and the tolerance factor. The crystal structures of LG, LGM82, and LSGM8282 are illustrated in Figure 4. The $GaO_6$ octahedral in LG and LGM82 were observed to be tilted compared with the ideal perovskite structure such as LSGM8282. Glazer proposed a classification of the distortion based on octahedral tilts in perovskite structures.[20] According to Glazer's description, the orthorhombic space group *Pbnm* is represented as $a^+b^-c^-$. Namely, there are two tilt directions in LG and LGM82, representing as α and $\beta$, which are tilt angles around the *b* and *c* axes parallel to the $[110]_p$ and $[001]_p$ of proto-perovskite structure, respectively. The tilt angles estimated are listed in Table 3. The crystal structure of LGM82 was found to be relaxed by introducing $Mg^{2+}$ ion, because of the decreases in both the tilt angles of LGM82, compared with LG. The structure of LSGM8282 is furthermore relaxed, because the doubly introduced $Mg^{2+}$ and $Sr^{2+}$ ions result in the cubic perovskite structure. Namely, in the LG-based solid solutions, the substitutions of $Mg^{2+}$ ion, whose ionic radius is larger than that of $Ga^{3+}$ ion, and $Sr^{2+}$ ion, whose ionic radius is larger than that of $La^{3+}$ ion, seem to be effective in reducing the tilt angles of the $GaO_6$ octahedron.

It is well-known that the tolerance factor, *t*, is a relevant parameter for estimating the magnitude of distortion in a perovskite $ABO_3$ structure. The tolerance factor, t, is represented by

$$t = \frac{d_{AO}}{\sqrt{2}d_{BO}}$$

where $d_{AO}$ and $d_{BO}$ are mean A−O and B−O bond lengths, respectively. When the tolerance factor is close to unity, the distortion is reduced, and the perovskite is close to the cubic structure. The values calculated by using the analytical results are listed in Table 3. The tolerance factor approached unity by replacing $Ga^{3+}$ ion in LG with $Mg^{2+}$ ion, and attained $t = 1.0$ by furthermore replacing $La^{3+}$ ion in LGM82 with $Sr^{2+}$ ion. This

(20) Glazer, A. M. *Acta Crystallogr. A* **1975**, *A31*, 756.

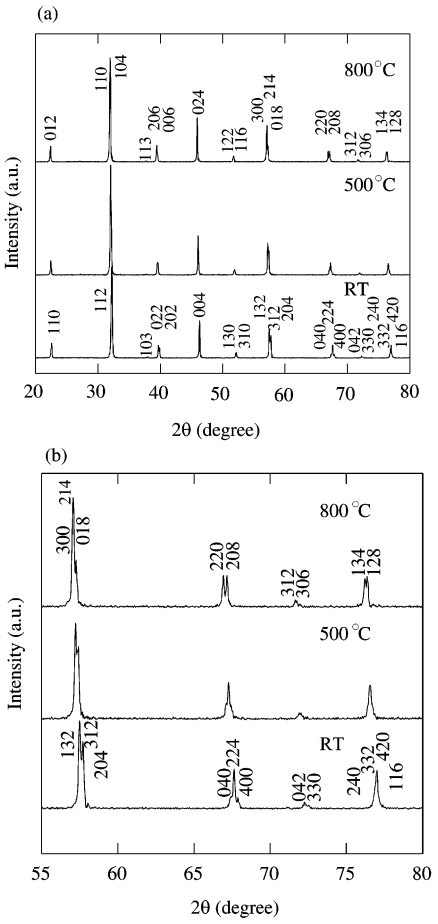


**Figure 7.** XRD patterns of $LaGa_{0.8}Mg_{0.2}O_{2.9}$ in the ranges (a) $20° \leq 2\theta \leq 80°$ and (b) $55° \leq 2\theta \leq 80°$ as a function of temperature.

means that the distortion of perovskite structure is reduced by substituting larger divalent ions such as $Mg^{2+}$ and $Sr^{2+}$ ions, although the oxygen vacancies are created. The tendency of the tolerance factors is consistent with that of the $GaO_6$ octahedral tilts. Consequently, LSGM8282 underwent a change into the ideal perovskite structure, and the oxygen vacancies became in disorder.

In addition to the structure refinements, the total conductivities, $\sigma$, and structural changes of LGM82 and LSGM8282 as a function of temperature were examined to obtain information on the high oxide ion conduction mechanism in LSGM. Figure 5 shows the total conductivities of LGM82 and LSGM8282 as a function of temperature. The total conductivities of LGM82 and LSGM8282 at high-temperature region were comparable to those of LSGM9182. The linear $\log\sigma$ vs $1/T$ plot for LSGM8282 was observed in the measured temperature range, whereas that for LGM82 broke at about 600 °C, and became parallel to that for LSGM8282 in the high-temperature region. These suggest that the phase transition occurs for LGM82 at about 600 °C, and the oxide ion conduction mechanism of LGM82 is similar to that of LSGM8282 at high temperature.

Figures 6 and 7 show XRD patterns of LSGM8282 and LGM82, respectively, as a function of temperature. The structural changes in LSGM8282 were hardly observed up to 800 °C. It was, therefore, expected that the oxygen vacancies were in disorder at 800 °C, and the disorder brought the high oxide ion conductivity in LSGM8282. On the other hand, the high-temperature XRD revealed that though the structure of LGM82 belonged to the orthorhombic space group *Pbnm* up to 500 °C, it belonged to the rhombohedral space group $R\bar{3}c$ or $R3c$ at 800 °C via phase transition from the fact that some XRD peaks based on the *Pbnm* disappeared or split. This is consistent with the temperature-dependence of electrical conductivity as shown in Figure 5. Provided that the disorder of oxygen vacancies gave rise to the high oxide ion conductivity in analogy with LSGM8282, the space group of LGM82 was supposed to be $R\bar{3}c$ with centrosymmetry at 800 °C.

## Conclusion

The crystal structures of LG, LGM82, and LSGM8282 analyzed by neutron powder diffraction were concluded as follows. The crystal structures of LG and LGM82 belong to the orthorhombic space group *Pbnm*, whereas that of LSGM8282 belongs to the cubic space group $Pm\bar{3}m$ and assumes the proto-perovskite structure. The results revealed that the substitutions of $Mg^{2+}$ ion (with larger ionic radius) for $Ga^{3+}$ ion and $Sr^{2+}$ ion (with larger ionic radius) for $La^{3+}$ ion in LG reduced the distortion of perovskite structure. Consequently, the symmetry of perovskite structure went up, and the oxygen vacancies became in disorder. From the results of high-temperature XRD and electrical conductivity, it seemed that the disorder induced the high oxide ion conductivities in LSGM8282 and LGM82 at 800 °C. The structural analyses of these compounds at operating temperatures of 800 °C or below are in progress to clarify the oxide ion conduction mechanism in detail.

CM030294Y